PERGAMON

International Journal of Plasticity 19 (2003) 1297–1319

INTERNATIONAL JOURNAL OF Plasticity

www.elsevier.com/locate/ijplas

Plane stress yield function for aluminum alloy sheets—part 1: theory

F. Barlat[a,b,*], J.C. Brem[a], J.W. Yoon[b,c], K. Chung[d], R.E. Dick[e], D.J. Lege[a], F. Pourboghrat[g], S.-H. Choi[f], E. Chu[h]

[a]*Materials Science Division, Alcoa Technical Center, 100 Technical Drive, Alcoa Center, PA 15069-0001, USA*

[b]*Center for Mechanical Technology and Automation, University of Aveiro, P-3810 Aveiro, Portugal*

[c]*Marc development group, MSC Software Corporation, 260 Sheridan Av., Palo Alto, CA 94306, USA*

[d]*Department of Materials Science and Engineering, College of Engineering, Seoul National University, 56-1, Shinlim-Dong, Kwanak-Ku, Seoul, 151-742, South Korea*

[e]*Rigid Packaging Design and Development, Alcoa Technical Center, 100 Technical Drive, Alcoa Center, PA 15069-0001, USA*

[f]*POSCO Technical Research Laboratories, 699, Kumho-Dong, Kwangyang-Shi, Cheonam, 545-090, South Korea*

[g]*Deptartment of Mechanical Engineering, Michigan State University, 2241 Engineering Building, East Lansing, MI 48824, USA*

[h]*Forming and Machining Platform, Alcoa Technical Center, 100 Technical Drive, Alcoa Center, PA 15069-0001, USA*

Received in final revised form 19 April 2002

Abstract

A new plane stress yield function that well describes the anisotropic behavior of sheet metals, in particular, aluminum alloy sheets, was proposed. The anisotropy of the function was introduced in the formulation using two linear transformations on the Cauchy stress tensor. It was shown that the accuracy of this new function was similar to that of other recently proposed non-quadratic yield functions. Moreover, it was proved that the function is convex in stress space. A new experiment was proposed to obtain one of the anisotropy coefficients. This new formulation is expected to be particularly suitable for finite element (FE) modeling simulations of sheet forming processes for aluminum alloy sheets.

Keywords: B: Anisotropic materials; B. Constitutive modeling; B. Metallic materials; C. Mechanical testing; Yield function

* Corresponding author. Tel.: +1-724-337-3920; fax: +1-724-337-2044.
E-mail address: frederic.barlat@alcoa.com (F. Barlat).

0749-6419/03/$ - see front matter
PII: S0749-6419(02)00019-0

1. Introduction

Over the years, yield functions were developed to describe the plastic anisotropy of sheet metals, for instance, Hill (1948, 1979, 1990, 1993). Other references can be found in the work by Barlat et al. (1997b) and Banabic (2000). Some of these yield functions were particularly intended for aluminum alloy sheets (Barlat and Lian, 1989; Barlat et al., 1991a; Karafillis and Boyce, 1993; Barlat et al., 1997a,b). The strain rate potential is another possible concept that can describe plastic anisotropy (Hill, 1987; Barlat et al., 1993,1998; Barlat and Chung, 1993). However, the strain rate potential is not discussed in this paper.

The yield functions referenced above have been implemented into some finite element (FE) codes to simulate sheet forming processes (Chung and Shah, 1992; Yoon et al., 1999; Tucu and Neale, 1999; Inal et al., 2000; Worswick and Finn, 2000). Although theoretical problems still remain, particularly, in relation to the rotation and distortion of the initial anisotropic reference frame (Tucu et al., 1999), reasonable assumptions have led to very successful forming process simulations (Yoon et al., 1999). It is the perception of the authors that, at the present time, one of the most accurate anisotropic yield functions for aluminum and its alloys is the function denoted Yld96 (for instance, Lademo, 1999; Lademo et al., 1999). This yield function (Barlat et al., 1997a,b) takes seven parameters into account in the plane stress condition. These parameters can be computed from σ_0, σ_{45}, σ_{90}, r_0, r_{45} and r_{90}, the uniaxial yield stresses and r values (width-to-thickness strain ratio in uniaxial tension) measured at 0, 45 and 90° from the rolling direction, and σ_b the balanced biaxial yield stress measured with the bulge test. There are three problems associated with Yld96 with respect to FE simulations:

- There is no proof of convexity, which is an important requirement in numerical simulations to ensure the uniqueness of a solution.
- The derivatives are difficult to obtain analytically which is inconvenient again for FE simulations.
- The plane stress implementation in FE codes does not provide any particular problems and leads to good simulation results. However, for full stress states, some numerical problems, which might be difficult to solve because of the relative complexity of the Yld96 formulation, have been encountered (Becker, 1998; Szabo, 2001).

The objective of this paper is to explore better incompressible anisotropic plasticity formulations that can guarantee convexity, make FE implementation and application simpler, and take σ_0, σ_{45}, σ_{90}, r_0, r_{45}, r_{90} and σ_b into account for plane stress.

2. General considerations

If an isotropic function is convex with respect to the principal stresses, then this function is also convex with respect to the stress components expressed in any set of

material axes (see proof in the Appendix). For instance, Φ_1 and Φ_2 are two isotropic functions, convex with respect to the three principal stresses and, consequently, with respect to the six components of the stress tensor expressed in any material frame

$$\Phi_1 = |s_1 - s_2|^a + |s_2 - s_3|^a + |s_3 - s_1|^a = 2\bar{\sigma}^a \tag{1}$$

$$\Phi_2 = |s_1|^a + |s_2|^a + |s_3|^a = \frac{2^a + 2}{3^a}\bar{\sigma}^a \tag{2}$$

In Eqs. (1) and (2), $\bar{\sigma}$ is the effective stress, "a" is a material coefficient, and s_1, s_2 and s_3 are the principal values of the stress deviator $\mathbf{s}$. The yield criterion (1), introduced by Hershey (1954) and Hosford (1972), is particularly suitable to account for the crystal structure (bcc, fcc) of an isotropic material. This function was extended to orthotropic anisotropy using a linear transformation $\mathbf{L}$ on the Cauchy stress tensor $\boldsymbol{\sigma}$ (Barlat et al., 1991a).

$$\mathbf{s}' = \mathbf{L}.\boldsymbol{\sigma} \tag{3}$$

The principal values of the transformed deviator $\mathbf{s}'$ are used in place of s_1, s_2, s_3 in Eqs. (1) and (2) to obtain anisotropic yield functions. Because a linear transformation on the stresses does not affect the convexity (Rockafellar, 1970), these anisotropic functions are also convex. Karafillis and Boyce (1993) used a combination of Φ_1 and Φ_2 as an alternate yield function,

$$\Phi_3 = (1 - c)\Phi_1 + c\frac{3^a}{2^{a-1} + 1}\Phi_2 = 2\bar{\sigma}^a \tag{4}$$

in which c is a coefficient. All of the above yield functions are acceptable anisotropic convex yield functions when used with the transformed deviator $\mathbf{s}'$. Karafillis and Boyce showed that $\mathbf{L}$ can take the symmetry of the material into account. For orthotropic materials, in a 6 by 6 notation, $\mathbf{L}$ reduces to

$$\mathbf{L} = \begin{bmatrix} L_{11} & L_{12} & L_{13} & & & \\ L_{21} & L_{22} & L_{23} & & & \\ L_{31} & L_{32} & L_{33} & & & \\ & & & L_{44} & & \\ & & & & L_{55} & \\ & & & & & L_{66} \end{bmatrix} \tag{5}$$

In the above matrix, zeros fill the missing spots. However, in order to ensure independence of the hydrostatic pressure, Karafillis and Boyce use the three conditions (for $k = 1$, 2 and 3)

$$L_{1k} + L_{2k} + L_{3k} = 0 \tag{6}$$

Since in addition, they assumed the diagonal symmetry for **L**, they had only six available parameters and four for a plane stress state, with the additional isotropic coefficient c. This does not satisfy the objective stated in the previous section because seven parameters are necessary to account for σ_0, σ_{45}, σ_{90}, r_0, r_{45}, r_{90} and σ_b. This is the reason why the yield function Yld96 was developed. However, Yld96 was not obtained from a linear transformation in the manner described above, and convexity could not be proven.

In general, a yield function written in terms of the deviatoric stress tensor fulfills the pressure independence condition. Therefore, another linear transformation could be:

$$\mathbf{X} = \mathbf{C}.\mathbf{s} \tag{7}$$

where s is the deviatoric stress tensor and X the linearly transformed stress tensor. Since there are 5 independent deviatoric stress components, the most general linear transformation from a five-dimensional space to a six-dimensional space, assuming orthotropic symmetry, with axes **x**, **y** and **z**, can be written as:

$$\begin{bmatrix} X_{xx} \\ X_{yy} \\ X_{zz} \\ X_{yz} \\ X_{zx} \\ X_{xy} \end{bmatrix} = \begin{bmatrix} C_{11} & C_{12} & 0 & & & \\ C_{21} & C_{22} & 0 & & & \\ C_{31} & C_{32} & 0 & & & \\ & & & C_{44} & & \\ & & & & C_{55} & \\ & & & & & C_{66} \end{bmatrix} \begin{bmatrix} s_{xx} \\ s_{yy} \\ s_{zz} \\ s_{yz} \\ s_{zx} \\ s_{xy} \end{bmatrix} \tag{8}$$

with no conditions on the C_{ij}. This gives 9 independent coefficients for the general case and 7 for plane stress. However, applied to plane stress conditions, only one coefficient (C_{66}) is available to account for σ_{45} and r_{45}. Therefore, this more general linear transformation does not appear to fulfill the objective of this work.

An exhaustive review of the theories dealing with plastic anisotropy was given by Życzkowski (1981). The type of linear transformations described by Eq. (3) was first presented by Sobotka (1969). In order to introduce more coefficients into anisotropic yield function, Cazacu and Barlat (2001) have proposed a general approach based on the theory of representation of anisotropic functions. In the present work, however, the more restrictive approach based on linear transformations was used because it allows a much simpler treatment of the convexity condition. Additional coefficients in the context of linear transformations are obtained by using two transformations associated to two different isotropic yield functions. This idea can be generalized to κ linear transformations, $\mathbf{X}^{(\kappa)} = \mathbf{C}^{(\kappa)}\mathbf{s}$, and κ isotropic yield functions, φ_κ. The resulting yield function, Φ_4, is given by

$$\Phi_4 = \sum_{\kappa} \varphi_\kappa\left(\mathbf{X}^{(\kappa)}\right) = 2\bar{\sigma}^a \tag{9}$$

Because there are three principal stresses in the full stress state, isotropic functions must contain a certain number of terms (for instance, Φ_1 and Φ_3 contain 3 and 6

terms, respectively), which could produce too many constraints to achieve the objective stated in Section 1. With the same number of coefficients, it is easier with a simple functional form to account for all the input data than with a more complex form. However, for plane stress, isotropic functions can be simpler because there are only two principal stresses. Therefore, this paper deals with the plane stress case only.

3. Yield function Yld2000–2d

An isotropic yield function that reduces to the function proposed by Hershey (1954) and Hosford (1972) in Eq. (1) can be simply

$$\phi = \phi' + \phi'' = 2\bar{\sigma}^a \tag{10}$$

where

$$\phi' = |s_1 - s_2|^a \quad \phi'' = |2s_2 + s_1|^a + |2s_1 + s_2|^a \tag{11}$$

Because, as mentioned above, a plane stress state can be described by two principal values only, ϕ' and ϕ'' are two isotropic functions since it is possible to permute the (in-plane) indices 1 and 2 in each function. Therefore, Eqs. (10) and (11) describe the yield function ϕ as a particular case of Eq. (9) with $\kappa = 2$. For the anisotropic case, the linear transformations reduce to

$$\begin{bmatrix} X'_{xx} \\ X'_{yy} \\ X'_{xy} \end{bmatrix} = \begin{bmatrix} C'_{11} & C'_{12} & 0 \\ C'_{21} & C'_{22} & 0 \\ 0 & 0 & C'_{66} \end{bmatrix} \begin{bmatrix} s_{xx} \\ s_{yy} \\ s_{xy} \end{bmatrix},$$
$$\begin{bmatrix} X''_{xx} \\ X''_{yy} \\ X''_{xy} \end{bmatrix} = \begin{bmatrix} C''_{11} & C''_{12} & 0 \\ C''_{21} & C''_{22} & 0 \\ 0 & 0 & C''_{66} \end{bmatrix} \begin{bmatrix} s_{xx} \\ s_{yy} \\ s_{xy} \end{bmatrix} \tag{12}$$

or, using

$$\mathbf{T} = \begin{bmatrix} 2/3 & -1/3 & 0 \\ -1/3 & 2/3 & 0 \\ 0 & 0 & 1 \end{bmatrix} \tag{13}$$

they become

$$\mathbf{X}' = \mathbf{C}'.\mathbf{s} = \mathbf{C}'.\mathbf{T}.\boldsymbol{\sigma} = \mathbf{L}'.\boldsymbol{\sigma}$$
$$\mathbf{X}'' = \mathbf{C}''.\mathbf{s} = \mathbf{C}''.\mathbf{T}.\boldsymbol{\sigma} = \mathbf{L}''.\boldsymbol{\sigma} \tag{14}$$

The anisotropic yield function is given by Eq. (10) where

$$\phi' = \left|X'_1 - X'_2\right|^a \quad \phi'' = \left|2X''_2 + X''_1\right|^a + \left|2X''_1 + X''_2\right|^a \tag{15}$$

It reduces to the isotropic expression when the matrices $\mathbf{C}'$ and $\mathbf{C}'$ are both taken as the identity matrix so that $\mathbf{X}' = \mathbf{X}'' = \mathbf{s}$. Because ϕ' depends on $X'_1 - X'_2$, only three coefficients are independent in C′. In this work, the condition $C'_{12} = C'_{21} = 0$ is imposed, but it is worth noting that $C'_{12} = C'_{21} = 1$ is an acceptable condition that leads to $\mathbf{X}' = \boldsymbol{\sigma}$ if $C'_{11} = C'_{22} = 2$. For convenience in the calculation of the anisotropy parameters (see Appendix), the coefficients of $\mathbf{L}'$ and $\mathbf{L}''$ can be expressed as follows

$$\begin{bmatrix} L'_{11} \\ L'_{12} \\ L'_{21} \\ L'_{22} \\ L'_{66} \end{bmatrix} = \begin{bmatrix} 2/3 & 0 & 0 \\ -1/3 & 0 & 0 \\ 0 & -1/3 & 0 \\ 0 & 2/3 & 0 \\ 0 & 0 & 1 \end{bmatrix} \begin{bmatrix} \alpha_1 \\ \alpha_2 \\ \alpha_7 \end{bmatrix}$$
$$\begin{bmatrix} L''_{11} \\ L''_{12} \\ L''_{21} \\ L''_{22} \\ L''_{66} \end{bmatrix} = \frac{1}{9} \begin{bmatrix} -2 & 2 & 8 & -2 & 0 \\ 1 & -4 & -4 & 4 & 0 \\ 4 & -4 & -4 & 1 & 0 \\ -2 & 8 & 2 & -2 & 0 \\ 0 & 0 & 0 & 0 & 9 \end{bmatrix} \begin{bmatrix} \alpha_3 \\ \alpha_4 \\ \alpha_5 \\ \alpha_6 \\ \alpha_8 \end{bmatrix} \tag{16}$$

where all the independent coefficients α_k (for k from 1 to 8) reduce to 1 in the isotropic case. Only seven coefficients are needed to account for the seven input data mentioned above. There are several possibilities to deal with the eighth coefficient, for instance, assuming $C''_{12} = C''_{21}$ or $L''_{12} = L''_{21}$, or use another input data. This additional input data can be the ratio $r_b = \dot{\varepsilon}_{yy}/\dot{\varepsilon}_{xx}$, which characterizes the slope of the yield surface in balanced biaxial tension $(\sigma_{yy} = \sigma_{xx})$. This parameter, which is denoted r_b by analogy with the r value obtained in uniaxial tension, can be determined with three different methods: experimentally measured, calculated with another yield function, for instance Yld96, or computed from a polycrystal model if the crystallographic texture of the material is known.

The principal values of $\mathbf{X}'$ and $\mathbf{X}''$ are

$$X_1 = \tfrac{1}{2}\left(X_{xx} + X_{yy} + \sqrt{(X_{xx} - X_{yy})^2 + 4X_{xy}^2}\right)$$
$$X_2 = \tfrac{1}{2}\left(X_{xx} + X_{yy} - \sqrt{(X_{xx} - X_{yy})^2 + 4X_{xy}^2}\right) \tag{17}$$

with the appropriate indices (prime and double prime) for each stress. Assuming the associated flow rule, the normal direction to the yield surface, which is needed to calculate the strain rates (or strain increments), is given by

$$\frac{\partial \phi}{\partial \boldsymbol{\sigma}} = \frac{\partial \phi'}{\partial \mathbf{X}'} \cdot \frac{\partial \mathbf{X}'}{\partial \boldsymbol{\sigma}} + \frac{\partial \phi''}{\partial \mathbf{X}''} \cdot \frac{\partial \mathbf{X}''}{\partial \boldsymbol{\sigma}} = \frac{\partial \phi'}{\partial \mathbf{X}'} \cdot \mathbf{L}' + \frac{\partial \phi''}{\partial \mathbf{X}''} \cdot \mathbf{L}'' \tag{18}$$

In the calculation of the derivatives, there are two singular cases, namely when $X'_1 = X'_2$ and $X''_1 = X''_2$ (see Appendix). However, the normal directions to the yield surface can still be obtained for these two special cases.

Appendix section A1 gives $\frac{\partial \phi'}{\partial \mathbf{X}'}$ and $\frac{\partial \phi''}{\partial \mathbf{X}''}$ and Appendix section A2 proves the convexity of the yield function. The calculation of the yield function coefficients is performed using the Newton–Raphson (NR) procedure. Guidelines needed for deriving the NR equations and obtaining the numerical solution are given in Appendix section A3.

4. Applications

4.1. Validation on binary Al–Mg alloy sheet sample

In this paper, **x**, **y** and **z** represent the rolling, transverse and normal directions of the sheet, respectively. In order to show the flexibility of the formulation, the model was applied to the case of a binary aluminum alloy containing 2.5 wt.% of magnesium (Mg). Because Mg is in solid solution in the aluminum matrix at room temperature, the alloy is a single phase material, i.e., an ideal polycrystal. The yield surface of this sheet sample was measured (Barlat et al., 1997b) using stacked sheet specimens and the testing method developed by Tozawa and Nakamura (1972), Tosawa (1978). The (111) and (200) pole figures were obtained using X-ray diffraction techniques from which the distribution of grain orientations was derived from standard mathematical tools (Bunge, 1982). This crystallographic texture was used as input for the full constraints Taylor (1938) / Bishop and Hill (1951a,b) polycrystal model (TBH) to compute the plane stress yield surface. Fig. 1a shows the experimental yield surface together with the TBH predictions. In this figure, all the stresses are normalized by the uniaxial yield stress in the rolling direction. In spite of the fact that some experimental points are questionable due to the delamination of few specimens (mainly uniaxial compression), the agreement between experiments and polycrystal predictions is remarkable. The very high stress level in pure shear $(\sigma_y = -\sigma_x,\ \sigma_{xy} = 0)$ and simple shear $\sigma_{xy},\ \sigma_y = \sigma_x = 0$ is very well captured by the polycrystal model.

For the phenomenological modeling of the yield surface using Yld2000–2d, the normalized uniaxial yield stresses at 0, 45 and 90° from the rolling direction, and the balanced biaxial yield stress were all assumed to be equal to 1.0. Under these conditions, most of the anisotropic yield functions would lead to an isotropic response of the material as illustrated by the dashed line in Fig. 1b using the functions proposed by Barlat and Lian (1989) and Barlat et al. (1991a,b). However, the new formulation Yld2000–2d has enough flexibility to use as input, in addition to flow stresses, uniaxial r values which can be much smaller than the isotropic r value (1.0). Fig. 1b shows the yield surface obtained for $r_0 = 0.20$, $r_{45} = 0.28$, $r_{90} = 0.20$ and $r_b = 1.0$, r_0, r_{45} and r_{90} were measured using uniaxial tension tests, separately from the yield surface measurements. These values are small because the material was processed using a non-standard route. The balance biaxial value, r_b, was computed

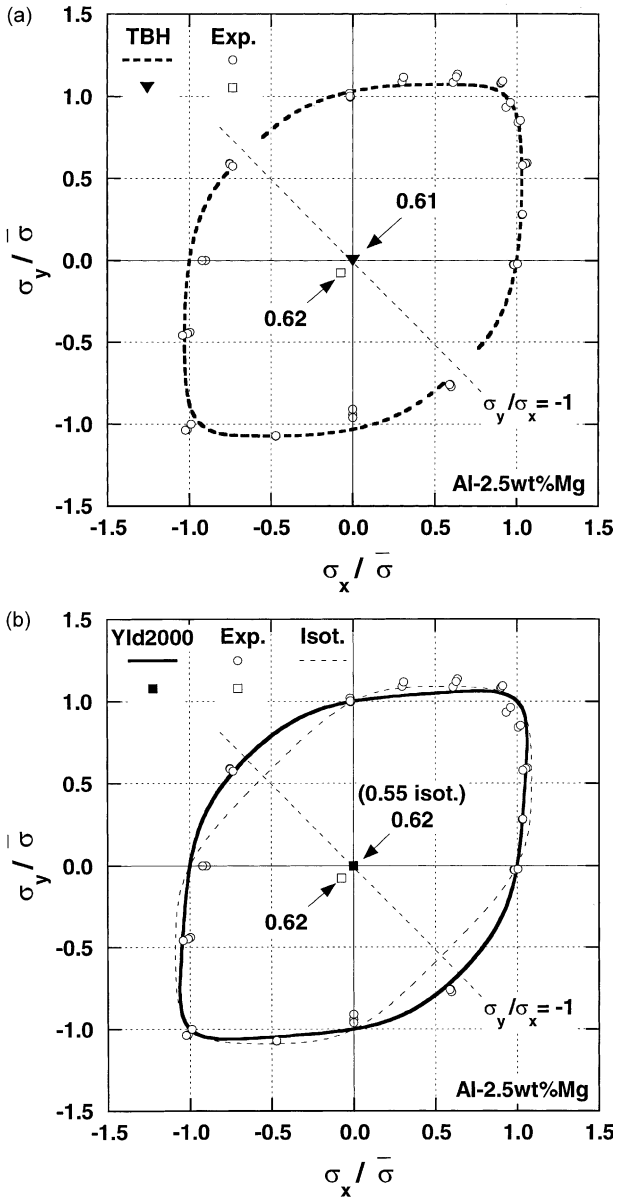

Fig. 1. Normalized yield surface for an Al–2.5 wt.% Mg binary sheet sample. Open circles denote experimental planar locus $(\sigma_{xy} = 0)$ and the open square denotes the maximum experimental simple shear stress $(\sigma_{xx} \approx \sigma_{yy} \approx 0)$. (a) Dash line $(\sigma_{xy} = 0)$ and solid triangle $(\sigma_{xx} \approx \sigma_{yy} \approx 0)$ denote polycrystal TBH predictions. (b) The solid line (planar locus, $\sigma_{xy} = 0$) and full square (maximum simple shear stress, $\sigma_{xx} \approx \sigma_{yy} \approx 0$) denote Yld2000-2d predictions using $\sigma_0 = \sigma_{45} = \sigma_{90} = \sigma_b$ and $r_0 = 0.20, r_{45} = 0.28, r_{90} = 0.20, r_b = 1.0$. Dash line represents isotropic response (isot.).

from a polycrystal model. Using these r values, the yield surface predicted using Yld2000–2d is in excellent agreement with both experimental and polycrystal yield surfaces. This example shows the flexibility of the function and its ability to reproduce polycrystal as well as experimental results very well. Moreover, it provides an excellent validation of the formulation.

4.2. Application to commercial aluminum alloys

The yield function Yld2000-2d was applied to two different aluminum alloy sheet samples: AA2090-T3 (Al–2.2Li–2.7Cu–0.12Zr) and AA6022-T4 (Al–1.25Si–0.75Mn–0.6Cu–0.57Mg–0.13Fe) sheet samples. The former material, used for aerospace applications, is a strongly textured sheet exhibiting more anisotropy than the latter, which is an autobody sheet.

The tension and bulge test experiments for a nominal 1.6 mm thick sample of AA2090-T3 sheet were reported elsewhere (Barlat et al., 1991b). In this work, through-thickness disk compression tests were conducted using 12.7 mm diameter specimens (Fig. 2). The specimens were loaded in compression using either dry film graphite (aerosol) or Teflon sheets (2.54 μm thick) as lubrication between the faces of the specimens and points of contact with the upper and lower platens of the compression test fixture. The diameters both parallel and perpendicular to the rolling direction of the sheet and thickness were measured for each specimen prior to and after deformation. From the respective initial and final measurements made for each test specimen, the true strains in the thickness direction ε_z, parallel ε_x and perpendicular ε_y to the rolling direction of the sheet were calculated as:

$$\varepsilon = \ln\ (\text{final dimension}/\text{initial dimension}) \tag{19}$$

Specimen shapes observed after deformation are shown in Fig. 2. The maximum load P_m, lubrication type used during loading for each of the compression tests, $\varepsilon_x, \varepsilon_y, \varepsilon_z$, along with the sum of the three strains measured for each specimen $\sum \varepsilon_\alpha = \varepsilon_x + \varepsilon_y + \varepsilon_z$ are listed in Table 1 for a selected number of specimens after deformation.

Theoretically, assuming constancy of volume, the sum of the strains $\sum \varepsilon_\alpha$ should be zero. However, this table shows that this sum is small, but not equal to zero. It

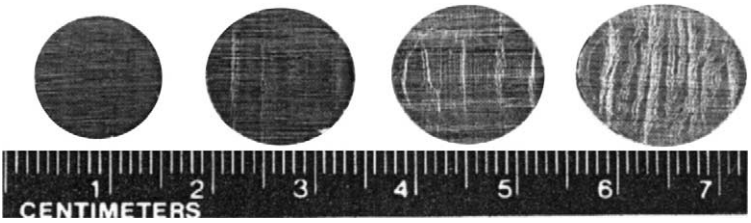

Fig. 2. Compression dick specimens for AA2090-T3 using different lubricants and at different thickness strains (ε_z). From left to right, undeformed, graphite at $\varepsilon_z = -0.261$, Teflon at $\varepsilon_z = -0.243$ and Teflon at $\varepsilon_z = -0.329$.

Table 1
Selected disk compression test results for AA2090-T3

ID	Lub.	P_m (kN)	ε_X	ε_y	ε_z	$\Sigma\varepsilon_\alpha$
1	Graphite	88.9	0.179	0.123	−0.280	0.022
2	Graphite	88.9	0.169	0.117	−0.261	0.025
3	Graphite	88.8	0.166	0.121	−0.269	0.018
4	Graphite	89.0	0.142	0.108	−0.234	0.016
5	Graphite	88.8	0.152	0.129	−0.264	0.017
6	Teflon	82.4	0.231	0.144	−0.311	0.064
7	Teflon	77.6	0.193	0.128	−0.243	0.078
8	Graphite	111.1	0.270	0.172	−0.409	0.033
9	Teflon	88.8	0.296	0.148	−0.329	0.115

can be speculated that the specimens do not deform strictly homogeneously. As observed in the table, the sums calculated for the specimens tested with the dry film graphite lubricant are closer to zero than the sums determined for the samples tested using the Teflon sheet lubricant. A possible reason for this discrepancy is the extensive transverse cracking (Fig. 2) evident on the surfaces of the Teflon lubricated specimens after deformation. For these specimens, the strains have exceeded the forming limit. These cracks are included in the final longitudinal measurement (ε_x) and have increased the overall strain level measured in the longitudinal direction x.

In Fig. 3, the transverse strains (ε_y) were plotted as a function of the longitudinal strains (ε_x) and a linear fit for all the graphite-lubricated-only specimens were performed to model the experimental points. The value of r_b was defined as the slope of the linear fit for the specimens deformed using the graphite lubricant. The experimental value of this parameter was found to be:

$$r_b = \mathrm{d}\varepsilon_y/\mathrm{d}\varepsilon_x = 0.67 \tag{20}$$

The data obtained with Teflon as a lubricant were not included in the analysis because the specimens were deformed beyond failure. Although the deformation of disks at low strains could have been made using Teflon as a lubricant as well, the measurements made with the dry film graphite were believed to be reliable and friction was expected to be low and roughly isotropic.

The other input data and the yield function coefficients are listed in Tables 2 and 3, respectively. Fig. 4 shows the experimental normalized yield stress and r value anisotropy (a and b respectively) for AA2090-T3 and predictions of these properties using Yld2000-2d and Yld96. Three methods were used to calculate the coefficients of Yld2000-2d, using either r_b measured experimentally, calculated either with Yld96 or assuming $L''_{12} = L''_{21}$. Fig. 5 shows the tricomponent yield surfaces for this material predicted with the Yld2000-2d yield function using r_b determined experimentally or calculated with Yld96. The Yld2000-2d yield function appears to be at least as accurate as Yld96 based on uniaxial r value and yield stress anisotropy predictions. The yield surfaces predicted with the two methods mentioned above are slightly different.

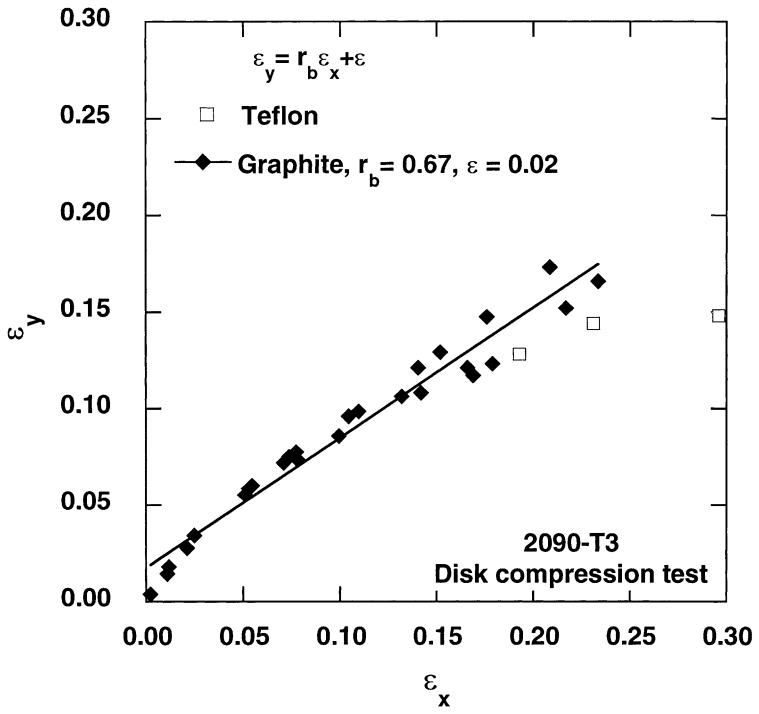

Fig. 3. Transverse ε_y vs. longitudinal ε_x strains in the disk compression test with different lubricants.

Table 2
Normalized yield stress and r values for AA2090-T3 and AA6022-T4

Material	σ_0	σ_{45}	σ_{90}	σ_b	r_0	r_{45}	r_{90}	Exp. r_b	Y1d96 r_b
2090-T3	1.000	0.811	0.910	1.035	0.21	1.58	0.69	0.67	0.33
6022-T4	0.994	0.962	0.948	1.000	0.70	0.48	0.59	–	1.36

Table 3
Anistotropy coefficients for AA2090-T3 and AA6022-T4. Exponent a is 8 for all material as recommended by Logan and Hosford (1980) for fcc materials

Material	Method	α_1	α_2	α_3	α_4	α_5	α_6	α_7	α_8
2090-T3	Exp. r_b	0.4865	1.3783	0.7536	1.0246	1.0363	0.9036	1.2321	1.4858
2090-T3	Yld96 r_b	0.6066	1.2472	0.5973	1.0079	1.0488	0.9675	1.2308	0.5130
2090-T3	$L''_{12} = L''_{21}$	0.3788	1.4712	0.8452	1.0289	1.0243	0.8452	1.2314	1.4747
6022-T4	Yld96 r_b	0.9370	1.0335	0.8452	1.0534	1.0107	0.9370	0.9594	1.1826
6022-T4	$L''_{12} = L''_{21}$	0.9355	1.0350	0.9337	1.0539	1.0102	0.9337	0.9594	1.1828

Table 4

			q_x	q_y
0° tension	2/3	−1/3	$1-r_0$	$2+r_0$
9.0° tension	−1/3	2/3	$2+r_{90}$	$1-r_{90}$
Balanced biaxial tension	−1/3	−1/3	$1+2r_b$	$2+r_b$

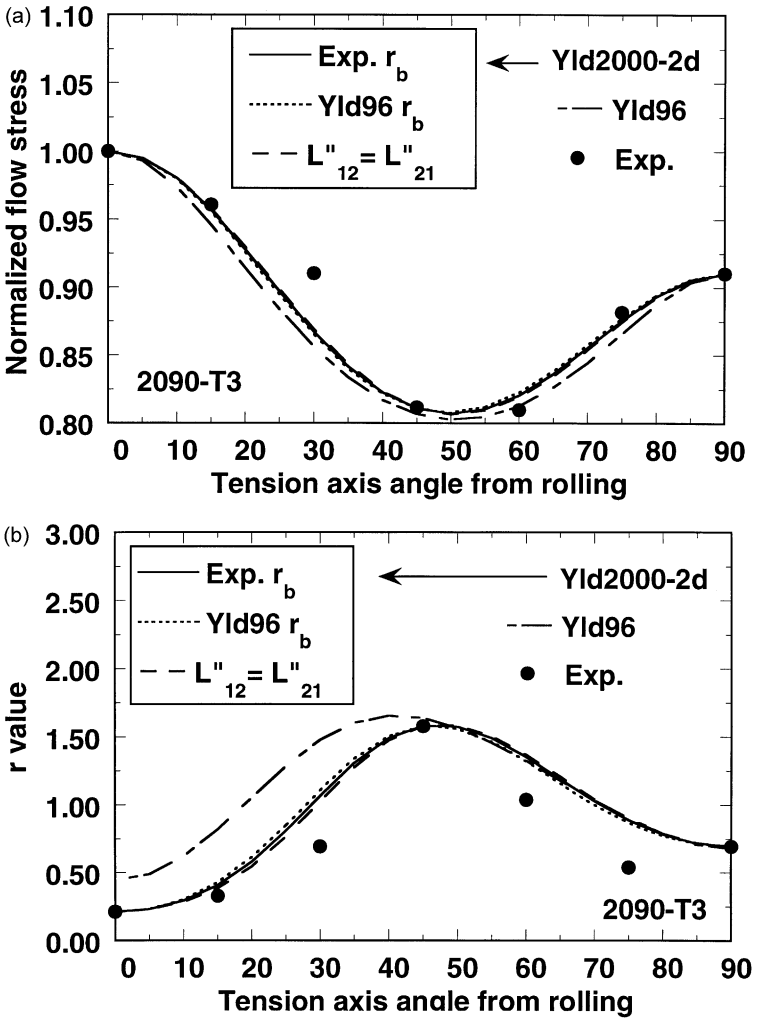

Fig. 4. Anistropy of uniaxial yield stress normalized by 0° uniaxial yield stress (a) and of r value (b) for AA2090-T3, experimentally measured and predicted with Yld2000-2d (experimental r_b), Yld2000-2d (Yld96 r_b), Yld2000-2d ($L''_{12}=L''_{21}$) and Yld96.

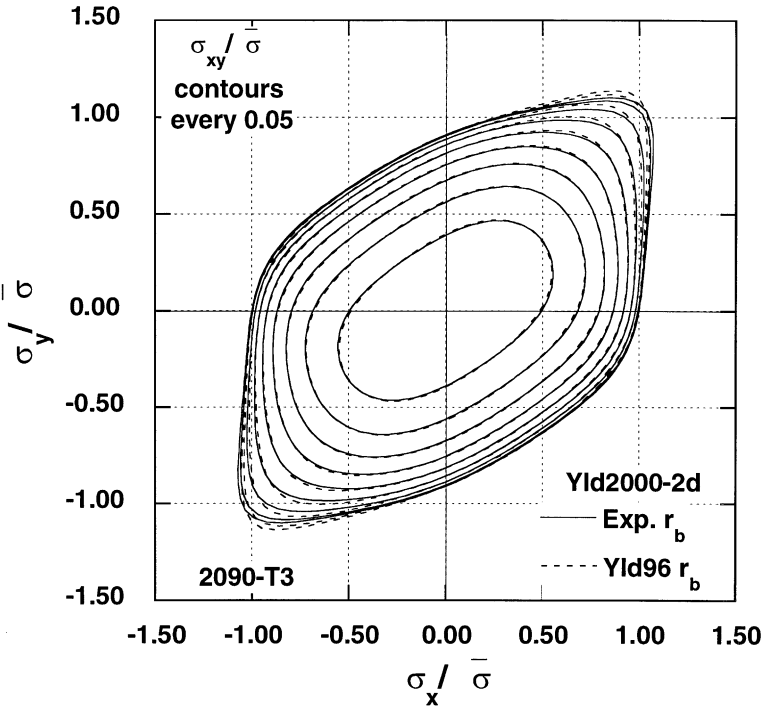

Fig. 5. Tricomponent yield surface for AA2090-T3 predicted with Yld2000-2d (experimental r_b) and Yld2000-2d (Yld96 r_b).

For the AA6022-T4 sheet sample, the tension and bulge test experiments were reported elsewhere (Barlat et al., 1997a,b). The predicted results using Yld2000-2d (with r_b from Yld96 or $L''_{12} = L''_{21}$) and Yld96 lead to virtually the same tensile property anisotropy (Fig. 6a and b). In Fig. 7, only one yield surface was represented, Yld2000-2d using Yld96 r_b, because it could not be distinguished from the surface based on the other prediction (Yld96). The material data and yield function coefficients for this AA6022-T4 sheet sample are listed in Tables 2 and 3.

4.3. Discussion

In terms of material anisotropy characterization, there are two separate issues that should not be confused. The first one, which was the goal of this paper, is the issue of the yield function formulation. The second issue is about how experimental tests are processed and what kind of data is used to identify the material anisotropy. Strictly speaking, a yield function should use yield stresses and r values at yield. However, this is too restrictive and does not give a good idea of the material behavior for a larger strain range. Therefore, another approach (Barlat et al., 1997a,b) consists in using flow stresses up to a given amount of plastic work (corresponding to a given strain, for instance, corresponding to the uniform elongation in tension), and the r values defined as the slope of the incremental width and thickness strain

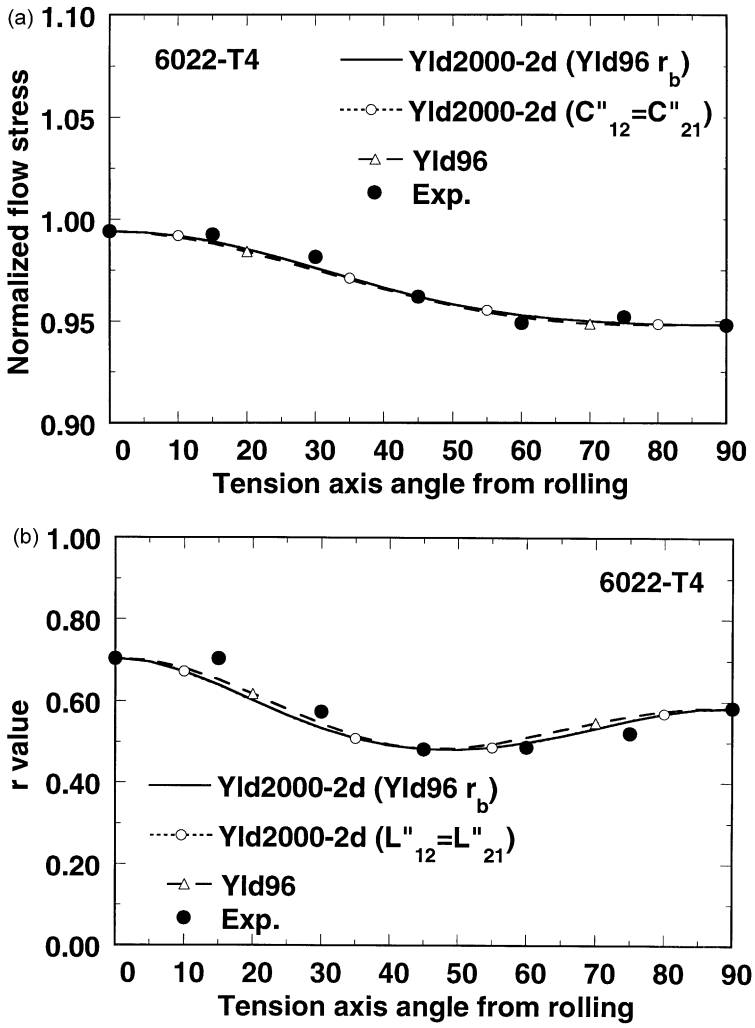

Fig. 6. Anisotropy of uniaxial yield stress normalized by the balanced biaxial yield stress (a) and of r value (b) for AA6022-T4, experimentally measured and predicted with Yld2000-2d (Yld96 r_b), Yld2000-2d ($L''_{12}=L''_{21}$) and Yld96.

measurements. This method is more attractive because, instead of giving a snapshot of the material state at yield, it gives an average material behavior for a significant strain range, although for the Al–Li alloy in this paper (Fig. 4), the 0.2% offset yield stresses were used. Also, r values were obtained from measurements of the tensile specimen after the test. This is because this Al–Li alloy exhibits serrated flow and it is not possible to measure reliable strains with extensometers.

It is worth noting at this point that, beside the examples reported in this work, many other aluminum alloy sheets of different compositions and temper conditions were tested in uniaxial tension. It was always observed that the slope of the incremental

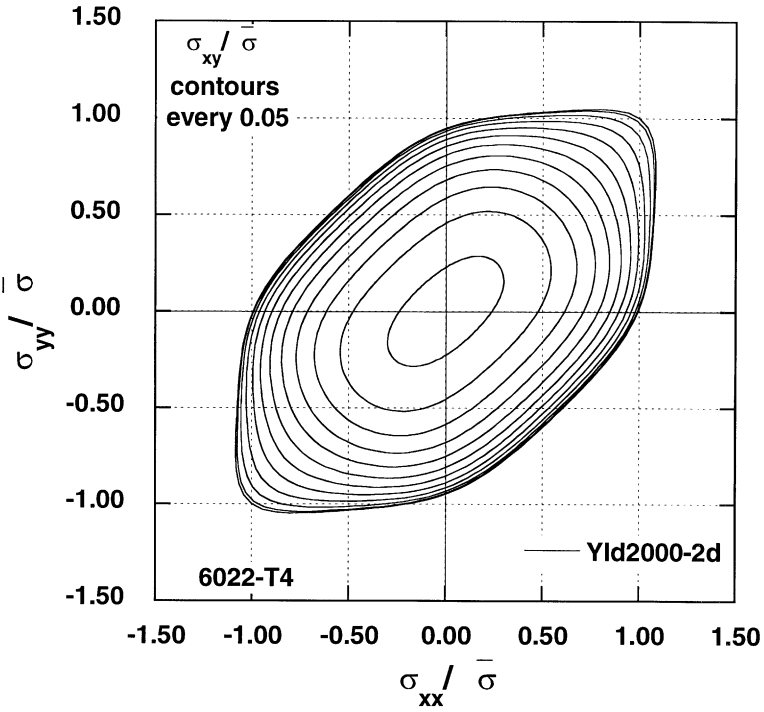

Fig. 7. Tricomponent yield surface for AA6022-T4 predicted with Yld2000-2d (Yld96 $_{rb}$).

width and thickness strains was linear, i.e., that the r value does not vary as much as it is often claimed, at least no more than within the range of experimental scatter.

These applications show that Yld2000-2d can be successfully applied either to weak and strong plastic anisotropy cases. As shown in the second part of this paper (Yoon and Barlat, in press), Yld2000-2d is much more efficient than Yld96 in FE simulations of sheet metal forming processes when the plane stress assumption is appropriate, because of the relative simplicity in its mathematical form.

5. Conclusions

The plane stress yield function Yld2000-2d was proposed and validated with experimental and polycrystal data obtained on a binary Al–2.5 wt.%Mg alloy sheet. This yield function provides a simpler formulation than Yld96 with at least the same accuracy. Its convexity is proven, and its implementation into FE codes appears to be straightforward. An efficient Newton–Raphson procedure was developed to numerically calculate the yield function coefficients using experimental data collected from a few tests only, three uniaxial tension tests in different orientations and one balanced biaxial bulge test. An experimental method, the disk compression test, was developed to measure a material parameter needed to calculate the yield function coefficients. However,

other methods can be used to evaluate this parameter if this new experiment cannot be performed. Yld2000-2d should be very well received by FE implementers and users for numerical simulations of aluminum sheet forming processes because of its accuracy and simplicity.

The model presented in this work was particularized to the case of aluminum alloys and orthotropic symmetry but, in fact, the method demonstrated in this paper is quite general. The principal aspect of this work is to use isotropic yield functions and, for anisotropy cases, replace the principal stresses by principal transformed stresses obtained from several linear transformations. The method can be applied to different materials with other symmetries, with pressure dependent materials or materials exhibiting a strength differential effect. Moreover, the model can be used in combination with anisotropic hardening rules, for instance as a substitute to the von Mises norm to express yield surface distortion (François, 2001).

The next challenge is to develop the full stress state yield function Yld2000-3d, equivalent to Yld2000-2d in terms of simplicity of formulation and accuracy. Such a yield function is needed for applications where full stress states are required, i.e., bending, springback, or when solid elements are needed in sheet forming, and in the entire area of bulk forming.

Acknowledgements

The authors would like to thank Dr. R.C. Becker (Lawrence Livermore National Laboratory) who provided the motivation to conduct this work and Dr. M.E. Karabin, Alcoa Technical Center, for a thorough review of the manuscript.

Appendix

A1. Yield surface normal

The gradient of the stress potential ϕ (yield function) leads to the strain rate. It is worth noting that, because this potential includes σ_{xy} and σ_{yx}, the strain rate is given by

$$\begin{aligned}\dot{\varepsilon}_{xx} &= \dot{\lambda}\frac{\partial\phi}{\partial\sigma_{xx}}\\ \dot{\varepsilon}_{yy} &= \dot{\lambda}\frac{\partial\phi}{\partial\sigma_{yy}}\\ \dot{\varepsilon}_{xy} &= \frac{\dot{\lambda}}{2}\frac{\partial\phi}{\partial\sigma_{xy}}\end{aligned} \tag{A1.1}$$

where $\dot{\lambda}$ is a proportionality factor.

A1.1. Derivative of ϕ'

The derivatives can be calculated provided the following quantity is not equal to zero.

$$\Delta' = \left(X'_{xx} - X'_{yy}\right)^2 + 4X'_{xy}2 \tag{A1.2}$$

A1.1.1. General case. This is the case where $\Delta' \neq 0$ or $X'_1 \neq X'_2$ or $\left(X'_{xx} \neq X'_{yy} \text{ or } X'_{xy} \neq 0\right)$

$$\frac{\partial \phi'}{\partial X'_{\alpha\beta}} = \frac{\partial \phi'}{\partial X'_1}\frac{\partial X'_1}{\partial X'_{\alpha\beta}} + \frac{\partial \phi'}{\partial X'_2}\frac{\partial X'_2}{\partial X'_{\alpha\beta}} \tag{A1.3}$$

where α and β denote indices for x and y.

$$\begin{aligned}
\frac{\partial \phi'}{\partial X'_1} &= a\left|X'_1 - X'_2\right|^{a-1}\operatorname{sign}\left(X'_1 - X'_2\right) = a\left(X'_1 - X'_2\right)^{a-1} \\
\frac{\partial \phi'}{\partial X'_2} &= -a\left|X'_1 - X'_2\right|^{a-1}\operatorname{sign}\left(X'_1 - X'_2\right) = -a\left(X'_1 - X'_2\right)^{a-1}
\end{aligned} \tag{A1.4}$$

$$\begin{aligned}
\frac{\partial X'_1}{\partial X'_{xx}} &= \frac{1}{2}\left(1 + \frac{X'_{xx} - X'_{yy}}{\sqrt{\Delta'}}\right) & \frac{\partial X'_2}{\partial X'_{xx}} &= \frac{1}{2}\left(1 - \frac{X'_{xx} - X'_{yy}}{\sqrt{\Delta'}}\right) \\
\frac{\partial X'_1}{\partial X'_{yy}} &= \frac{1}{2}\left(1 - \frac{X'_{xx} - X'_{yy}}{\sqrt{\Delta'}}\right) & \frac{\partial X'_2}{\partial X'_{yy}} &= \frac{1}{2}\left(1 + \frac{X'_{xx} - X'_{yy}}{\sqrt{\Delta'}}\right) \\
\frac{\partial X'_1}{\partial X'_{xy}} &= \frac{2X'_{xy}}{\sqrt{\Delta'}} & \frac{\partial X'_2}{\partial X'_{xy}} &= -\frac{2X'_{xy}}{\sqrt{\Delta'}}
\end{aligned} \tag{A1.5}$$

A1.1.2. Singular case. This is the case where $\Delta' = 0$ or $X'_1 = X'_2$ (or $X'_{xx} = X'_{yy}$ and $X'_{xy} = 0$ simultaneously). Any direction is a principal direction. Therefore, it is possible to choose the set of principal directions that is superimposed with the anisotropy axes, which leads to

$$\begin{aligned}
\frac{\partial \phi'}{\partial X'_{xx}} &= \frac{\partial \phi'}{\partial X'_1} = 0 \\
\frac{\partial \phi'}{\partial X'_{yy}} &= \frac{\partial \phi'}{\partial X'_2} = 0 \\
\frac{\partial \phi'}{\partial X'_{xy}} &= 0
\end{aligned} \tag{A1.6}$$

A1.2. Derivative of ϕ''

A1.2.1. General case. This is the case where $\Delta'' \neq 0$ or $X''_1 \neq X''_2$ or $\left(X''_{xx} \neq X''_{yy} \text{ or } X''_{xy} \neq 0\right)$

$$\frac{\partial \phi''}{\partial X''_{\alpha\beta}} = \frac{\partial \phi''}{\partial X''_1}\frac{\partial X''_1}{\partial X''_{\alpha\beta}} + \frac{\partial \phi''}{\partial X''_2}\frac{\partial X''_2}{\partial X''_{\alpha\beta}} \tag{A1.7}$$

where α and β denote indices for x and y.

$$\frac{\partial\phi''}{\partial X_1''} = a\left|2X_2'' + X_1''\right|^{a-1}\mathrm{sign}\left(2X_2'' + X_1''\right) + 2a\left|2X_1'' + X_2''\right|^{a-1}\mathrm{sign}\left(2X_1'' + X_2''\right)$$
$$\frac{\partial\phi''}{\partial X_2''} = 2a\left|2X_2'' + X_1''\right|^{a-1}\mathrm{sign}\left(2X_2'' + X_1''\right) + a\left|2X_1'' + X_2''\right|^{a-1}\mathrm{sign}\left(2X_1'' + X_2''\right) \quad \text{(A1.8)}$$

$$\begin{aligned}
\frac{\partial X_1''}{\partial X_{xx}''} &= \frac{1}{2}\left(1 + \frac{X_{xx}'' - X_{yy}''}{\sqrt{\Delta''}}\right) & \frac{\partial X_2''}{\partial X_{xx}''} &= \frac{1}{2}\left(1 - \frac{X_{xx}'' - X_{yy}''}{\sqrt{\Delta''}}\right)\\
\frac{\partial X_1''}{\partial X_{yy}''} &= \frac{1}{2}\left(1 - \frac{X_{xx}'' - X_{yy}''}{\sqrt{\Delta''}}\right) & \frac{\partial X_2''}{\partial X_{yy}''} &= \frac{1}{2}\left(1 + \frac{X_{xx}'' - X_{yy}''}{\sqrt{\Delta''}}\right)\\
\frac{\partial X_1''}{\partial X_{xy}''} &= \frac{2X_{xy}''}{\sqrt{\Delta''}} & \frac{\partial X_2''}{\partial X_{xy}''} &= -\frac{2X_{xy}''}{\sqrt{\Delta''}}
\end{aligned} \quad \text{(A1.9)}$$

A1.2.2. Singular case. This is the case where $\Delta'' = 0$ or $X_1'' = X_2''$ $\left(\text{or } X_{xx}'' = X_{yy}'' \text{ and } X_{xy}'' = 0 \text{ simultaneously}\right)$. Any direction is a principal direction. Therefore, it is possible to choose the set of principal directions that is superimposed with the anisotropy axes and Eq. (A1.8) to calculate the partial derivatives

$$\begin{aligned}
\frac{\partial\phi''}{\partial X_{xx}''} &= \frac{\partial\phi''}{\partial X_1''}\\
\frac{\partial\phi''}{\partial X_{yy}''} &= \frac{\partial\phi''}{\partial X_2''} = \frac{\partial\phi''}{\partial X_1''}\\
\frac{\partial\phi''}{\partial X_{xy}''} &= 0
\end{aligned} \quad \text{(A1.10)}$$

A2. Convexity

A2.1. Convexity with respect to principal transformed stresses

A yield function is convex if its Hessian matrix **H**

$$H_{ij} = \frac{\partial^2\phi}{\partial X_i \partial X_j} \quad \text{(A2.1)}$$

is positive semi-definite, i.e., its principal values are not negative (Rockafellar, 1970).

A2.2.1. Convexity of ϕ'. The Hessian matrix for ϕ' is

$$\mathbf{H}' = \begin{bmatrix} h' & -h' \\ -h' & h' \end{bmatrix} \text{with } h' = a(a-1)\left|X'_1 - X'_2\right|^{a-2} \tag{A2.2}$$

Both eigenvalues, 0 and $2h'$, are not negative when "a" is larger than 1 which proves that ϕ' is convex.

A2.2.2. Convexity of ϕ''. The Hessian matrix for ϕ'' is

$$\mathbf{H}'' = \begin{bmatrix} h''_1 + 4h''_2 & 2h''_1 + 2h''_2 \\ 2h''_1 + 2h''_2 & 4h''_1 + h''_2 \end{bmatrix} \quad \text{with} \begin{cases} h''_1 = a(a-1)\left|2X''_2 + X''_1\right|^{a-2} \\ h''_2 = a(a-1)\left|2X''_1 + X''_2\right|^{a-2} \end{cases} \tag{A2.3}$$

Solving for the eigenvalues, it can be shown that the sum and the product of the eigenvalues are respectively equal to $5\left(h''_1 + h''_2\right)$ and $9h''_1h''_2$. These quantities are not negative when "a" is larger than 1, proving that ϕ'' is convex.

A2.2. Convexity with respect to non-principal stresses

If a yield function is convex with respect to the principal stress components, then it is convex with respect to the stress components expressed in a different (non-principal) reference frame. Lippman (1970) showed this result but for the sake of completeness, a proof follows. It is assumed that **X*** and **X**** represent the components of the stress tensor **X** expressed in principal axes (X_k) or in another (non-principal) reference frame ($X_{\alpha\beta}$), respectively, and f is a yield function, convex with respect to the principal values of **X** (X_k). The relationship between the components of **X**** and **X*** is:

$$\begin{bmatrix} X_{11} \\ X_{22} \\ X_{33} \\ X_{23} \\ X_{31} \\ X_{12} \end{bmatrix} = \begin{bmatrix} p_{11}^2 & p_{12}^2 & p_{13}^2 \\ p_{21}^2 & p_{22}^2 & p_{23}^2 \\ p_{31}^2 & p_{32}^2 & p_{33}^2 \\ p_{21}p_{31} & p_{22}p_{32} & p_{23}p_{33} \\ p_{31}p_{11} & p_{32}p_{12} & p_{33}p_{13} \\ p_{11}p_{21} & p_{12}p_{22} & p_{13}p_{23} \end{bmatrix} = \begin{bmatrix} X_1 \\ X_2 \\ X_3 \end{bmatrix} \tag{A2.4}$$

where p_{kl} represents the components of the transformation matrix **p** between the two reference frames. This equation corresponds to a linear transformation between the components of **X**** and **X***. Moreover, Rockafellar (1970) showed that a linear transformation on the variables does not alter the convexity of a function. Therefore, the yield function f, convex with respect to the components of **X***, is also convex with respect to the component of **X****. As an application, ϕ' and ϕ'' are convex functions of $X'_{\alpha\beta}$ and $X''_{\alpha\beta}$, respectively, when $a \geqslant 1$.

A2.3. Convexity with respect to stresses

Since a linear transformation of the variables does not change the convexity of a function, ϕ' and ϕ'' which are convex functions of $X'_{\alpha\beta}$ and $X''_{\alpha\beta}$, respectively, are also both convex functions of $\sigma_{\alpha\beta}$ because $\mathbf{X}'$ and $\mathbf{X}''$ represent two linear transforma-

tions of $\boldsymbol{\sigma}$. Moreover, ϕ, the sum of two convex functions, is also a convex function (Rockafellar, 1970) of the stresses $\sigma_{\alpha\beta}$.

A3. Anisotropy parameter calculation

A3.1. Coefficients α_1 to α_6

Three stress states, namely uniaxial tension along the rolling and the transverse directions, and the balanced biaxial stress state, provide six data points, σ_0, σ_{90}, σ_{b}, r_0, r_{90}, and r_{b}. r_{b} Defines the slope of the yield surface at the balanced biaxial stress state $\left(r_b = \dot{\varepsilon}_{yy}/\dot{\varepsilon}_{xx}\right)$. This ratio can be evaluated by performing compression of circular disks in the sheet normal direction and measuring the aspect ratio of the specimen after deformation as discussed above. r_{b} can also be estimated by calculations using either a polycrystal model or the yield function Yld96. The loading for each stress state can be characterized by the two deviatoric components, $s_x = \gamma\sigma$ and $s_y = \delta\sigma$. There are two equations to solve per stress state, one for the yield stress and the other for the r value.

$$F = \phi - 2(\bar{\sigma}/\sigma)^a = 0 \quad \text{satisfies the yield stress} \tag{A3.1}$$

$$G = q_x \frac{\partial \phi}{\partial s_{xx}} - q_y \frac{\partial \phi}{\partial s_{yy}} = 0 \quad \text{satisfies the } r \text{ value} \tag{A3.2}$$

The function ϕ can be rewritten as

$$\phi = \left|\alpha_1\gamma - \alpha_2\delta\right|^a + \left|\alpha_3\gamma + 2\alpha_4\delta\right|^a + \left|2\alpha_5\gamma + \alpha_6\delta\right|^a - 2(\bar{\sigma}/\sigma)^a = 0 \tag{A3.3}$$

where γ, δ, σ, q_x, and q_y for the tests mentioned above are given in Table 4.

The 6 coefficients α_k can be computed by solving the two Eqs. (A3.1) and (A3.2) expressed in the three stress states. These equations were obtained using the linear transformations with the C_{k1} (prime and double prime) coefficients, which are related to the α_k coefficients in the following way

$$\begin{aligned}
\alpha_1 &= C'_{11} \\
\alpha_2 &= C'_{22} \\
\alpha_3 &= 2C''_{21} + C''_{11} \\
2\alpha_4 &= 2C''_{22} + C''_{12} \\
2\alpha_5 &= 2C''_{11} + C''_{21} \\
\alpha_6 &= 2C''_{12} + C''_{22}
\end{aligned} \tag{A3.5}$$

The α_k coefficients were used because the yield function reduces to its isotropic form when all these coefficients are 1. The C_{k1} and L_{k1} coefficients are linear combinations of the α_k.

A3.2. Coefficients α_7 and α_8

Uniaxial tension tests loaded at 45° to the rolling direction give two data points, $\sigma = \sigma_{45}$ and $r = r_{45}$. The stress state is on the yield surface if the following equation is satisfied

$$F = \left|\frac{\sqrt{k_2'^2 + 4\alpha_7^2}}{2}\right|^a + \left|\frac{3k_1'' - \sqrt{k_2''^2 + 4\alpha_8^2}}{4}\right|^a + \left|\frac{3k_1'' + \sqrt{k_2''^2 + 4\alpha_8^2}}{4}\right|^a - 2\left(\bar{\sigma}/\sigma_{45}\right)^a = 0 \tag{A3.6}$$

where

$$k_2' = \frac{\alpha_1 - \alpha_2}{3}$$
$$k_1'' = \frac{2\alpha_5 + \alpha_6 + \alpha_3 + 2\alpha_4}{9}$$
$$k_2'' = \frac{2\alpha_5 + \alpha_6 - \alpha_3 - 2\alpha_4}{3} \tag{A3.7}$$

The associated flow rule can be expressed as

$$G = \frac{\partial\phi}{\partial\sigma_{xx}} + \frac{\partial\phi}{\partial\sigma_{yy}} - \frac{2a\bar{\sigma}^a}{\sigma(1 + r_{45})} = 0 \tag{A3.8}$$

The Newton–Raphson numerical procedure is used to solve for the eight α_k coefficients simultaneously. The two matrices $\mathbf{L}'$ and $\mathbf{L}''$ (Section 2) are completely defined with these eight coefficients.

References

Banabic, D., 2000. Anisotropy in sheet Metals. In: Banabic, D. (Ed.), Formability of Metallic Materials. Springer, Berlin, p. 119.

Barlat, F., Lian, J., 1989. Plastic behavior and stretchability of sheet metals. Part I: a yield function for orthotropic sheets under plane stress conditions. Int. J. Plasticity 5, 51–66.

Barlat, F., Becker, R.C., Hayashida, Y., Maeda, Y., Yanagawa, M., Chung, K., Brem, J.C., Lege, D.J., Matsui, K., Murtha, S.J., Hattori, S., 1997a. Yielding description of solution strengthened aluminum alloys. Int. J. Plasticity 13, 385–401.

Barlat, F., Chung, K., 1993. Anisotropic potentials for plastically deforming metals. Modelling and Simulation in Materials Science and Engineering 1, 403–416.

Barlat, F., Chung, K., Richmond, O., 1993. Strain rate potential for metals and its application to minimum work path calculations. Int. J. Plasticity 9, 51–63.

Barlat, F., Chung, K., Yoon, J.W., Pourboghrat, F., 1998. Plastic anisotropy modeling for sheet forming design applications. In: Khan, A.S. (Ed.), Proceedings 7th International Symposium on Plasticity and its Current Applications. Neat Press, Fulton, MD, pp. 301–304.

Barlat, F., Lege, D.J., Brem, J.C., 1991a. A six-component yield function for anisotropic materials. Int. J. Plasticity 7, 693–712.

Barlat, F., Lege, D.J., Brem, J.C., Warren, C.J., 1991b. Constitutive behavior for anisotropic materials and application to a 2090-T3 Al–Li alloy. In: Lowe, T.C., Rollett, A.D., Follansbee, P.S., Daehn, G.S. (Eds.), Modeling the Deformation of Crystalline Solids. TMS, Warrendale, PA, pp. 189–203.

Barlat, F., Maeda, Y., Chung, K., Yanagawa, M., Brem, J.C., Hayashida, Y., Lege, D.J., Matsui, K., Murtha, S.J., Hattori, S., Becker, R.C., Makosey, S., 1997b. Yield function development for aluminum alloy sheets. J. Mech. Phys. Solids 45, 1727–1763.

Becker, R.C., 1998. Private information, Alcoa Technical Center, Pennsylvania, December 1998.

Bishop, J.W.F., Hill, R., 1951a. A theory of the plastic distortion of a polycrystalline aggregate under combined stresses. Philos. Mag. 42, 414–427.

Bishop, J.W.F., Hill, R., 1951b. A theoretical derivation of the plastic properties of polycrystalline face-centered metals. Philos. Mag. 42, 1298–1307.

Bunge, H.J., 1982. Texture Analysis in Materials Science—Mathematical Methods. Butterworth, London.

Cazacu, O., Barlat, F., 2001. Generalization of Drucker's yield criterion to orthotropy. Mathematics and Mechanics of Solids 6, 613–630.

Chung, K., Shah, K., 1992. Finite element simulation of sheet forming for planar anisotropic metals. Int. J. Plasticity 8, 453–476.

François, M., 2001. A plasticity model with yield surface distortion for non-proportional loading. Int. J. Plasticity 17, 703–717.

Hershey, A.V., 1954. The plasticity of an isotropic aggregate of anisotropic face centred cubic crystals. J. Appl. Mech. Trans. ASME 21, 241–249.

Hill, R., 1948. A theory of the yielding and plastic flow of anisotropic metals. Proc. Roy. Soc. London A193, 281–297.

Hill, R., 1979. Theoretical plasticity of textured aggregates. Math. Proc. Cambridge Philos. Soc. 85, 179–191.

Hill, R., 1987. Constitutive dual potential in classical plasticity. J. Mech. Phys. Solids 35, 23–33.

Hill, R., 1990. Constitutive modelling of orthotropic plasticity in sheet metals. J. Mech. Phys. Solids 38, 405–417.

Hill, R., 1993. A user-friendly theory of orthotropic plasticity in sheet metals. Int. J. Mech. Sci. 35, 19–25.

Hosford, W.F., 1972. A generalized isotropic yield criterion. J. Appl. Mech. Trans. ASME 39, 607–609.

Inal, K., Wu, P.D., Neale, K.W., 2000. Simulation of earing in textured aluminum sheets. Int. J. Plasticity 16, 635–648.

Karafillis, A.P., Boyce, M.C., 1993. A general anisotropic yield criterion using bounds and a transformation weighting tensor. J. Mech. Phys. Solids 41, 1859–1886.

Lademo, O.G., 1999. Engineering Models of Rlastoplasticity and Fracture for Aluminum Alloys. PhD thesis, Norvegian Institute of Science and Technology, Trondheim, Norway, 1999.

Lademo, O.G., Hopperstad, O.S., Langseth, M., 1999. An evaluation of yield criteria and flow rules for aluminum alloys. Int. J. Plasticity 15, 191–208.

Lippman, H., 1970. Matrixungleichungen und die Konvexität der Fliessfläche. Zeit. Angew. Mech. 50, 134–137.

Logan, R.W., Hosford, W.F., 1980. Upper-bound anisotropic yield locus calculations assuming pencil glide. Int. J. Mech. Sci. 22, 419–430.

Rockafellar, R.T., 1970. Convex Analysis. Princeton University Press, Princeton, NY.

Sobotka, Z., 1969. Theory des plastischen fliessens von anisotropen körpern. Zeit. Angew. Math. Mech. 49, 25–32.

Szabo, L., 2001. Private communication at Euromech Colloquium 430, Formulations and Constitutive Laws for Very Large Strains, Prague, Czech Republic, October 2001.

Taylor, G.I., 1938. Plastic strains in metals. J. Institute of Metals 62, 307–324.

Tozawa, N., 1978. Plastic deformation behavior under the conditions of combined stress. In: Koistinen, D.P., Wang, N.M. (Eds.), Mechanics of Sheet Metal Forming. Plenum Press, New-York, pp. 81–110.

Tozawa, N., Nakamura, M., 1972. A biaxial compression testing method for thin sheets. Plasticity and Processing 13, 538–541.

Tucu, P., Neale, K.W., 1999. On the implementation of anisotropic yield functions into finite strain problems of sheet metal forming. Int. J. Plasticity 16, 701–720.

Tucu, P., Wu, P.D., Neale, K.W., 1999. Finite strain analysis of simple shear using recent anisotropic yield criteria. Int. J. Plasticity 16, 701–720.

Worswick, M.J., Finn, M.J., 2000. The numerical simulation of stretch flange forming. Int. J. Plasticity 16, 701–720.

Yoon, J.W., Barlat, F., in press. Plane stress yield function for aluminum alloy sheets—Part II: FE implementation. Int. J. Plasticity.

Yoon, J.W., Yang, D.Y., Chung, K., Barlat, F., 1999. A general elasto-plastic finite element formulation based on incremental deformation theory for planar anisotropy and its application to sheet metal forming. Int. J. Plasticity 15, 35–68.

Zyczkowski, M., 1981. Combined loadings at the level P of a point of a body. In: Combined Loadings in the Theory of Plasticity, Polish Scientific Publishers, Warsaw, Poland, p.87.